energies

MDPI

Article

Tidal Energy Flows between the Midriff Islands in the Gulf of California

Federico Angel Velazquez-Muñoz and Anatoliy Filonov *

Department of Physics, University of Guadalajara, Guadalajara 44100, Mexico; federico.velazquez@academicos.udg.mx
* Correspondence: anatoliy.filonov@cucei.udg.mx

Abstract: The Gulf of California has many regions of potential tidal-stream energy that have been identified and characterized using in-situ measurements and numerical ocean models. The Midriff Islands region has received particular attention due to its increased current speeds and high kinetic energy. This increase in energy can be seen in the formation of internal wave packets propagating for several hundred kilometers. Here we present a brief description of internal wave measurements travel towards the Northern Gulf and explore energy generation sites. In this paper we characterize the tidal inflow and outflow that passes throughout the Midriff Islands in the central part of the Gulf. We use a three-dimensional numerical ocean model that adequately reproduces the tidal flow and the increase in speed and kinetic energy between the islands. The current flow structure shows the highest velocity cores near the shore and far from the bottom. During the rising tide, the maximum current flow (~0.6 ms^{-1}) was found between Turón Island and San Lorenzo Island, from the surface to 200 m depth. When the currents flowed out of the Gulf, during the falling tide, the maximum negative current (−0.8 ms^{-1}) was found between Tiburon Island and Turón Island, from near the surface to 80 m depth. Although there are favorable conditions for power generation potential by tidal flows, the vertical variability of the current must be considered for field development and equipment installation sites.

Keywords: modeling of tidal energy flows; "in situ" assessment; gulf of California; Midriff archipelago

Citation: Velazquez-Muñoz, F.A.; Filonov, A. Tidal Energy Flows between the Midriff Islands in the Gulf of California. *Energies* **2021**, *14*, 621. https://doi.org/10.3390/en14030621

Academic Editor: Rodrigo Carballo Sánchez
Received: 1 December 2020
Accepted: 21 January 2021
Published: 26 January 2021

1. Introduction

Tidal energy is unevenly distributed in the different oceans. It tends to be concentrated near underwater sills and in narrow areas between islands. In these regions, strong tidal currents arise, which transform part of the energy of the barotropic tidal flow into its potential form, generating internal (baroclinic) tidal waves. These flows, together with the barotropic flow, create a complex picture of dynamics in certain regions of the ocean. Because internal waves create intense vertical movements, cause mixing of water layers, and contribute to the redistribution of nutrients from the depths of the ocean to the surface, they are being actively studied by scientists from different countries.

Large-amplitude internal tidal waves have been observed near submarine sills in many regions of the world, in particular in the Gulf of California (GC) [1–4], along the Pacific coast of Mexico, [5–8], as well as in many other regions of the world, such as in the Andaman [9–13] and Sulu Seas [14,15]. Previous authors [16] consider that in general, for the world ocean, the energy of the internal semidiurnal tide is 10–50% of that of the barotropic tide. The ratio of the energy of the baroclinic tide to that of the barotropic tide can be calculated from the following expression:

$$\zeta = \frac{\sum_{I=1}^{N} \delta_{IW_i}^2 h_i}{\delta_{BT}^2 H} \quad (1)$$

where $\delta^2_{IW_i}$ is the variance of the current fluctuation caused by internal tides at the corresponding level; δ^2_{BT} is the variance of the current due to the barotropic tide; h_i is the thickness of the i-th layer; and H is the bottom depth at the mooring, given by the equation:

$$H = \sum_{i-1}^{6} h_i \quad (2)$$

Studies [17] have estimated that in a mooring installed in the northern Gulf of California, the baroclinic tide receives up to 45% of the energy from the barotropic tide, which is close to the upper bound of the range suggested by [16], therefore the process by which these internal waves are generated must be a very important source of energy.

Internal tidal waves in the sill area of the GC have been characterized using satellite observations. [2] were the first to analyze Synthetic Aperture Radar (SAR) images in the GC, and based on a simple nonlinear model of the Korteweg-de-Vries equation (KdV), they determined that groups of short-period internal tidal waves with a semidiurnal periodicity were generated at San Esteban sill during spring tides. [18] also used satellite images to report on the initial stages of the distortion of the thermocline by tidal flows over San Esteban Sill.

Although the process of internal tides is well known and the propagation and disintegration of these internal waves has been studied, in order to identify particular high energy sites, an analysis of the vertical structure of marine currents is required in the areas where the most intense current flows occur. Herein we present the characterization of the vertical structure (in depth) of the current that passes between the Islands using the output data of a three-dimensional model. This place in the GC has been identified as one of the sites with the highest kinetic energy and it is necessary to identify the characteristics of the flow and determine the sites with the highest speed and energy of the current, which can occur in the deep or superficial layers.

In Section 2 we present an overview of the study region in the central Gulf of California, showing the islands and seamounts. In Section 3 we present the numerical model and the methodology used to quantify the physical flux variables in the vertical depth section between the islands. Finally, a description of numerical model results and the discussion is presented in Section 4, with conclusions in Section 5.

2. Study Area

Large amplitude internal tidal waves are generated in the sill area of the productive Gulf of California (GC), Mexico, which is located between an archipelago with several channels that separate the northern and the central regions (Figure 1). The tides in the GC are in co-oscillation with the Pacific Ocean and because of the length of the Gulf, they are almost resonant to the semidiurnal tidal frequency [19]. These topographic and dynamic features cause strong tidal currents in this area (up to 1.0 m s^{-1}), which release a large amount of turbulent kinetic energy that have an important impact on regional physics and biology [6,20,21]. In [22], the results of numerical modeling of the baroclinic currents generated by internal tides in the study area are discussed.

The region of the large midriff islands in the northern part of the GC is of great scientific interest as an area of concentration of tidal energy entering from the ocean. This part of the Gulf was the subject of active research in the 1980 by scientists from CICESE (Center for Scientific Research and Higher Education, Ensenada, Mexico) and the Scripps Institute of Oceanography, as part of the Pichicuco joint project to study the thermohaline structure and dynamics of the Gulf of California [1].

The Gulf of California stretches for almost 1500 km from northwest to southeast, between the Baja California Peninsula and western continental Mexico and is about 200 km wide. The circulation in the Gulf is strongly influenced by the processes in the straits connecting the Guaymas Basin with the northern part between 28° and 29° north latitudes. The islands of San Lorenzo, San Esteban and Tiburon, each about 15 km wide, shorten the

cross section of this part of the Gulf and dramatically increase the speed of tidal currents in this area. The westernmost Ballenas-Salsipuedes channel has a depth of more than 1600 m at its center. The central San Esteban channel is located between the islands of San Lorenzo and San Esteban and is the widest. There is also a third channel between the islands of San Esteban and Tiburon, which also plays a significant role in regional water exchange.

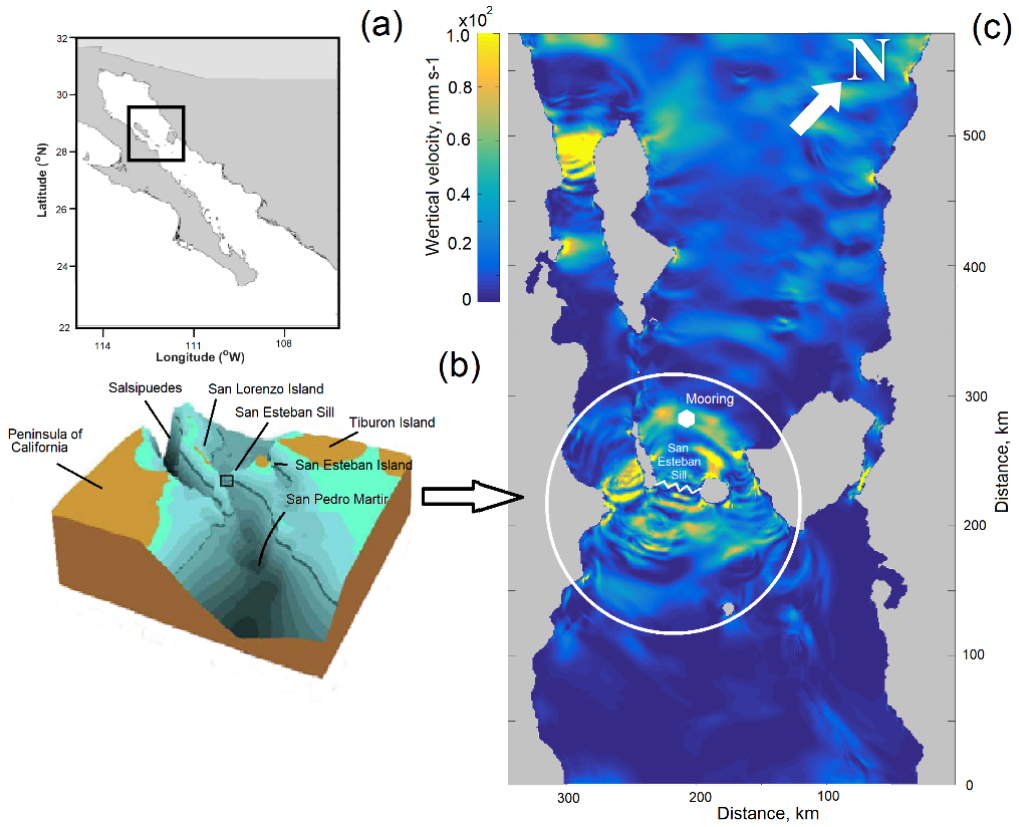

Figure 1. (**a**) Study area in the Gulf of California. (**b**) Islands and inter-island channels in the area of San Esteban Sill (courtesy of M. Lavin). The rectangle shows the location of the underwater sill. (**c**) Vertical component of the tidal current velocity in the study area, calculated using the POM model.

3. Methodology

3.1. Numerical Model

As mentioned above, the highest concentration of kinetic energy in the Gulf occurs in the Midriff Region, so the model configuration includes only this area with a relatively high resolution compared to other models [23,24]. For this experiment, we used the Princeton Ocean Model [25] that resolves the hydrostatic primitive equation under the Boussinesq approximation. The model uses a sigma coordinate system in the vertical direction, and the horizontal grid discretized in an Arakawa-C differencing scheme with Cartesian coordinates (x, y), with 1-km horizontal resolution and 41 sigma levels in the vertical direction. The initial conditions for velocity is zero and temperature and salinity are specified in the entire domain as a uniform profile with no horizontal variation in order to avoid pressure gradients.

The numerical domain (Figure 2a) has an open boundary condition at the left and right (southeast and northwest in the gulf). The x coordinate is aligned in the along-gulf direction and the y coordinate, in a cross-gulf direction, such that they are oriented toward the northwest and southwest, respectively. In the left boundary condition, we used a time-dependent tidal flow velocity as forcing while in the right boundary we used a radiation condition of the normal velocity component. The model simulation was for 30 days and reaches its dynamic equilibrium in the first 2 days. We analyze the most energetic day to

represent the general scenario for inflow and outflow currents, on the assumption that temporary variations only increase or decrease the intensity of the values but not the spatial variability in depth. For detailed numerical model validation, see [22].

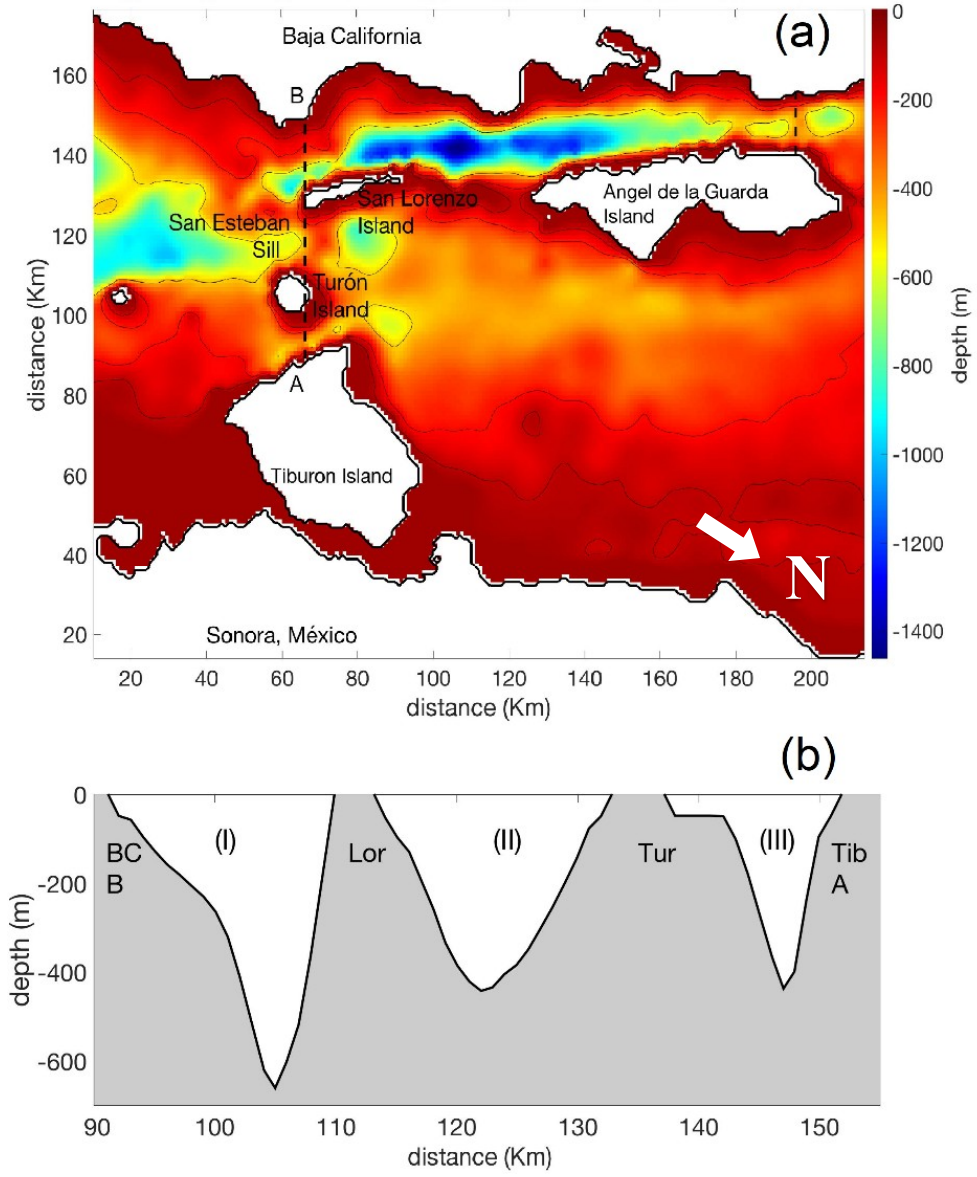

Figure 2. (**a**) Bathymetry of the Midriff archipelago area in the Gulf of California. The transect (A-B) used for quantitative estimates of the inflow and outflow of tidal energy. (**b**) depth profile showing the three sections across the Gulf along the transect (A-B), from Tiburón Island (Tib) to Baja California (BC), with Turón Island (Tur) and San Lorenzo Island (Lor) along the transect.

3.2. Variable Vertical Quantification for Each Depth Section

This contribution consists of quantifying and characterizing the flow passing through the narrow section between the Island in the middle of the Gulf, in the across-gulf line (Figure 2a) through the Island, which we consider as the entrance of the energy to the Northern Gulf. All the analyses are based on the along-gulf component of the three-dimensional ocean model velocity (u). Figure 2b, corresponds to a vertical section in depth from point A in Tiburón Island (Tib) to point B in Baja California (BC), passing through Turón Island (Tur) and San Lorenzo Island (Lor). As we have shown in Figure 2b, there are three sections between the Islands, numbered (I), (II) and (III), where we calculate the area

for each pass. Multiplying the velocity (u) in each node in the vertical cell area, we obtain the volumetric flux (Q), given by:

$$Q = u \cdot dy \cdot d\sigma, \tag{3}$$

where dy (=1000 m) is the numerical model horizontal resolution and dσ is the differential between numerical model sigma-levels, which is variable according to depth H.

In order to calculate the kinetic energy (KE) during the tidal cycle, we used the expression:

$$KE = \frac{1}{2}\rho_o u^2 \tag{4}$$

where ρ_o is the reference density and *u* the component of velocity in the direction along the gulf. In this case, the KE units are Joules per cubic meter (J m^{-3} = Kg m^2 s^{-2} m^{-3}) that can be multiplied by time (1 s) in order to obtain the KE in Watts per cubic meter (W m^{-3}).

3.3. Measurements on a Submerged Mooring

To estimate the kinetic energy flux in situ, we used the data of the currents measured on the mooring which was established to measure the disintegrations of internal waves generated by the barotropic tide at the San Esteban sill. The measurements were carried out at the end of September 2012 on board the R/V Francisco de Ulloa. The buoy was installed in Tiburon Basin (−122.87° E, 28.93° N) at a seabed depth of 430 m, 32 km northwest of San Esteban Sill (Figure 1c).

The ADCP Nortek 400 kHz was installed at 80 m depth measuring upward, at 17 levels every 30 s, with a cell size of 400 cm. Due to the lack of sufficient battery capacity of the device, measurements were conducted for only 2.25 days. A more detailed description of these measurements can be found in [21].

4. Results and Discussion

The general circulation in the Gulf of California during the tidal cycle produces an inflow and outflow that it is quite strong in some parts of the Gulf, reaching velocities greater than 1.0 m s^{-1} principally between the Midriff Islands in the Central and Northern Gulf [26–29]. When the tidal wave enters the Northwest area of the Gulf, it encounters a narrowing in the central gulf at the Midriff Islands of reduced width and depth, and therefore a considerable increase in velocity occurs.

One of the main processes that occur in the Gulf is the generation and propagation of internal waves [2] by the hydraulic jump caused by the passage of the tidal wave over the thresholds that extend between the mainland and the San Lorenzo, San Esteban and Tiburon Islands (dashed line in Figure 2). These internal waves propagate for several hundred kilometers, producing significant vertical movements that affect the biological productivity of the region. Our model implementation can reproduce the principal characteristics of internal wave patterns, shown in Figure 3 (upper panel), using the along-gulf velocity component, that it is produced by the internal hydraulic jump in the San Esteban and San Lorenzo Sills (Figure 3, lower panel). After accumulating large amounts of energy in the region between the Islands, the turbulent kinetic energy dissipates towards the Northern Gulf [6,22]. This internal wave generation is important and validated by the numerical model used, and much of the energy generated is due to baroclinic processes that are generally absent from the more-widely used 2D numerical ocean models.

4.1. Numerical Results

The reduced width and depth of the section through which the current flows produce a significant increase in speed, with a significant increase in kinetic energy, as shown in Figure 4, where the black arrows show the vertically-integrated velocity and the color tones correspond to the kinetic energy in units of J m^{-3}. The highest kinetic energy occurs between the islands.

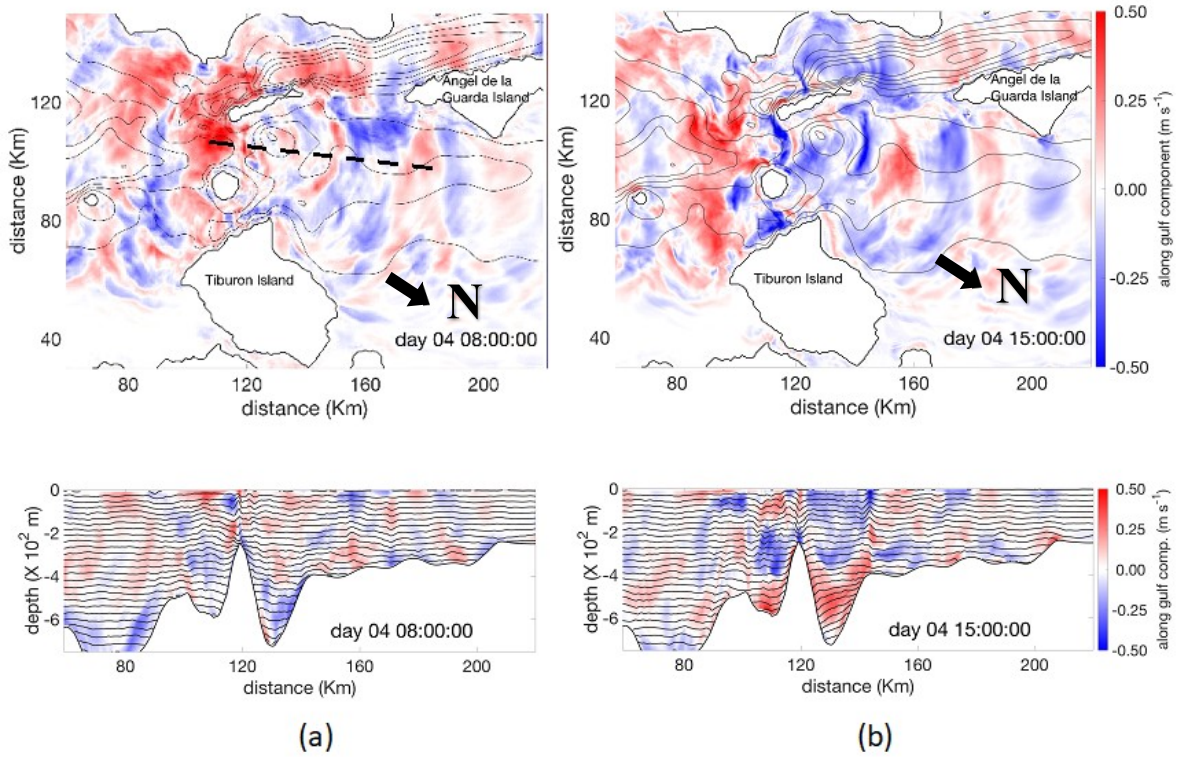

Figure 3. Maps of the surface (upper) and vertical (bottom) profiles of the along-gulf velocity component at two periods of model simulation (**a**) during the maximum entrance of tidal velocity (see red tones between the Islands) and (**b**) during the internal wave front propagation towards the northern gulf (see black arrow on high blue tones).

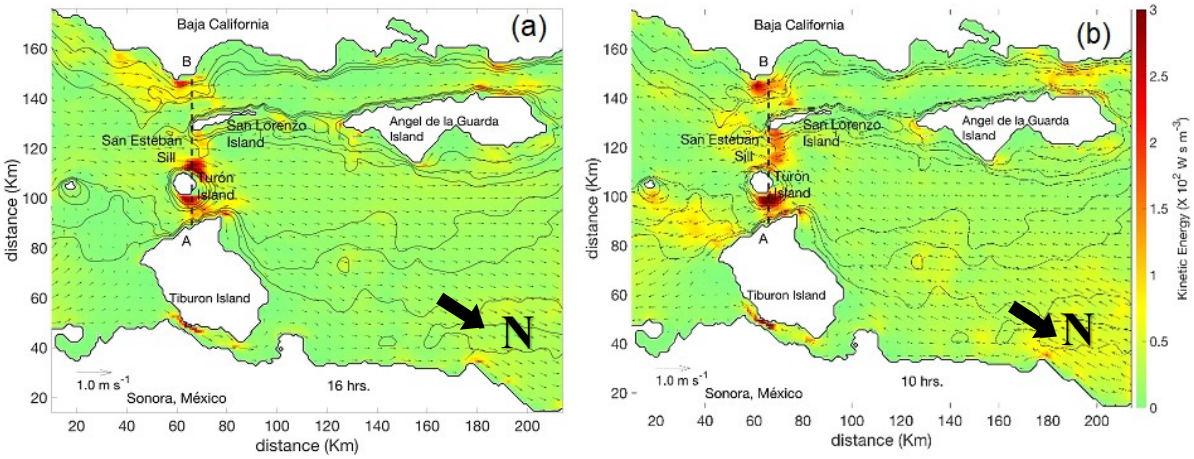

Figure 4. Maps of eddy kinetic energy and vertical integrated velocity in the Gulf of California Great Island Region for tidal inflow (**a**) and tidal out flow (**b**).

At the entrance to the Gulf, the width is ~193 km with a maximum depth of 4100 m, whereas between the islands the width is 55 km with three sections that have depths between 400 and 600 m (Figure 2). The area of each section is shown in Figure 2b, (I) between Tiburon Island and Turón Island is 2393.41 km^2, (II) between Turón Island and San Lorenzo Island is 4924.75 km^2 and, (III) between San Lorenzo Island and the coast of Baja California is 5580.73 km^2. Unexpectedly, the quantity of water that flows through each section is not proportional to its area.

Table 1 shows the calculated transport in Sverdrups (1 Sv = 10^6 m^3 s^{-1}) for the three sections during the inflowing and outflowing tidal current. In the numerical experiment, Section II is where the flows in both directions reach maximum values.

Table 1. Numerical values of the area and inflowing and outflowing transport in the depth sections between the Midriff Islands.

Section	Area (km^2)	Inflow Transport (Sv)	Outflow Transport (Sv)
I	2393	1.13	−1.05
II	4924	1.75	−2.07
III	5580	1.39	−1.53

Figure 5 shows two depth profiles of the velocity component along the Gulf at the three sections between the Islands. These velocity values correspond to times when the inflow (Figure 4a) and the outflow (Figure 4b) are at their maximum. Velocities vary throughout each section, with less intense currents occurring in Section III, with maximum values of 0.5 m s^{-1} in the upper depths and lower speeds of 0.1 m s^{-1} between 200 m depth and the bottom.

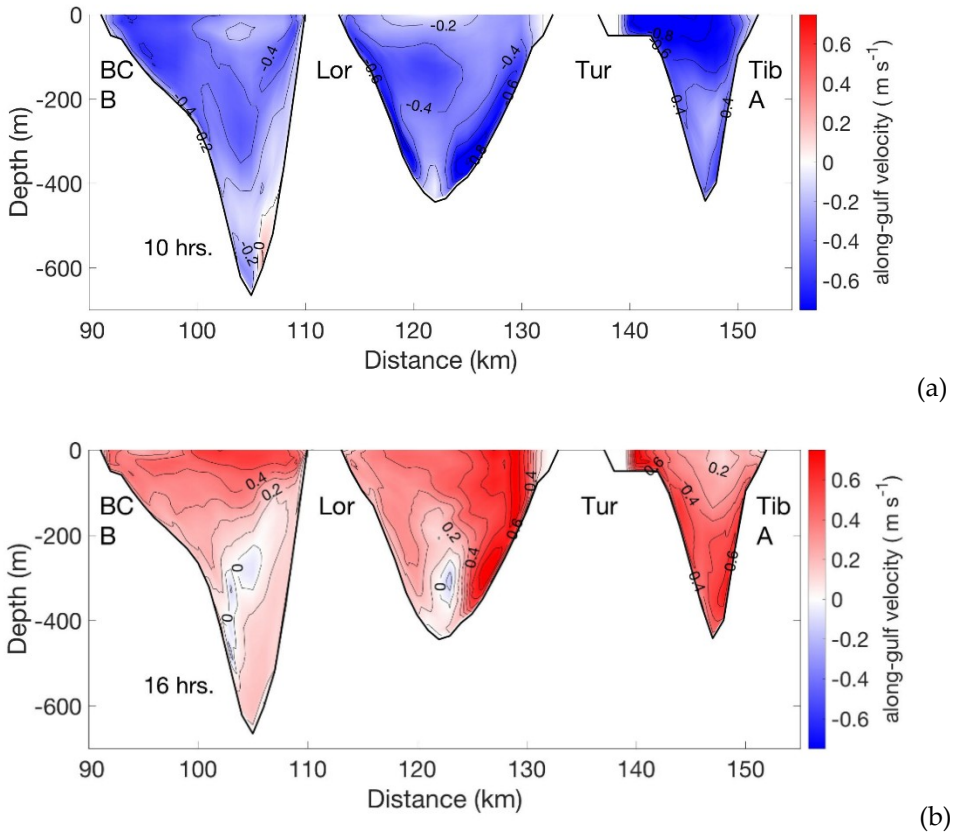

Figure 5. Depth Sections of the along-gulf component of velocity in the line along the transect A-B (see Figure 2a) for (**a**) inflow and (**b**) outflow.

The most intense currents were found in Section II, where values greater than 0.6 m s^{-1} occur on the Turón Island side from the surface to the bottom at 300 m deep. In Section I, the inflow is baroclinic during the rising tide. In our model experiment, the intense current flow towards the head of the Gulf in Section I occurs at the bottom and there is a soft core of outflow near the surface.

These three-dimensional velocity sections represent the values at each numerical grid node, however the velocity is in reference to the area of the cell to which it belongs, as it

represents a fluid variable termed the volume flux, Q, in $m^3\ s^{-1}$, seen for inflow (Figure 6 upper panel) and outflow (Figure 6 lower panel).

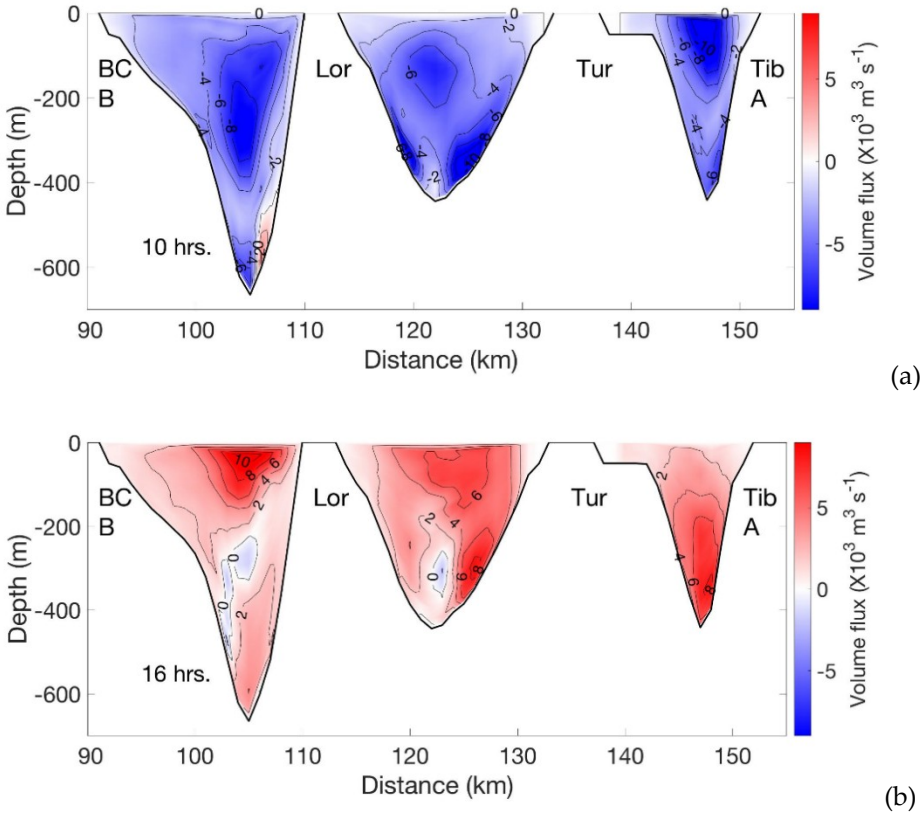

Figure 6. Same as Figure 5 but of the volumetric flux (Q) for (**a**) inflow and (**b**) outflow.

To characterize the kinetic energy produced in each of these sections through which the tidal wave passes in its progression towards the northern part of the Gulf, the kinetic energy (KE) of the along-gulf component current is shown in Figure 7, corresponding to the output data from the model, during the highest inflow and outflow. The results indicate that the highest energy is concentrated at the sides of the Islands, being greater at the side of Turón Island and near the coast of Baja California (see maps in Figures 4 and 7).

In the vertical direction, in the channel between Isla Tiburon and Isla Turón (Section III), the highest concentration of KE occurs in the upper-layers/deeper-layer when tidal currents are outflowing/inflowing (Figure 7a,b). In Section II, between Turón Island and San Lorenzo Island, there are two cores of lower KE, one in the deep part extending to the bottom at 400 m depth and another near the surface next to Turón Island between the surface and 100 m deep (Figure 7a,b). In Section III, between San Lorenzo Island and the Baja California peninsula, which is the channel with the largest area, the KE does not reach the values of the other two sections, and the cores of high KE are located near the surface, between the surface and 100 m deep for outflow, and between the surface and 300 m deep for inflow (Figure 7a,b). Contrary to the other sections, when the current is outflowing, only one core of intense KE is observed in Section II near the bottom.

Following [24] we calculated the Energy Production (EP) for a time lapse of one day. Figure 7c shows the mean EP in KW h for 24 h, where we can see that between San Lorenzo (LOR) and Turon (TUR) Islands (Section II) near the bottom and toward the Turon Island and between Turon (TUR) and Tiburon (TIB) Islands, next to the Turon Island shore showing high KE values between the Islands, These sites could be considered suitable for the installation of alternative energy production equipment.

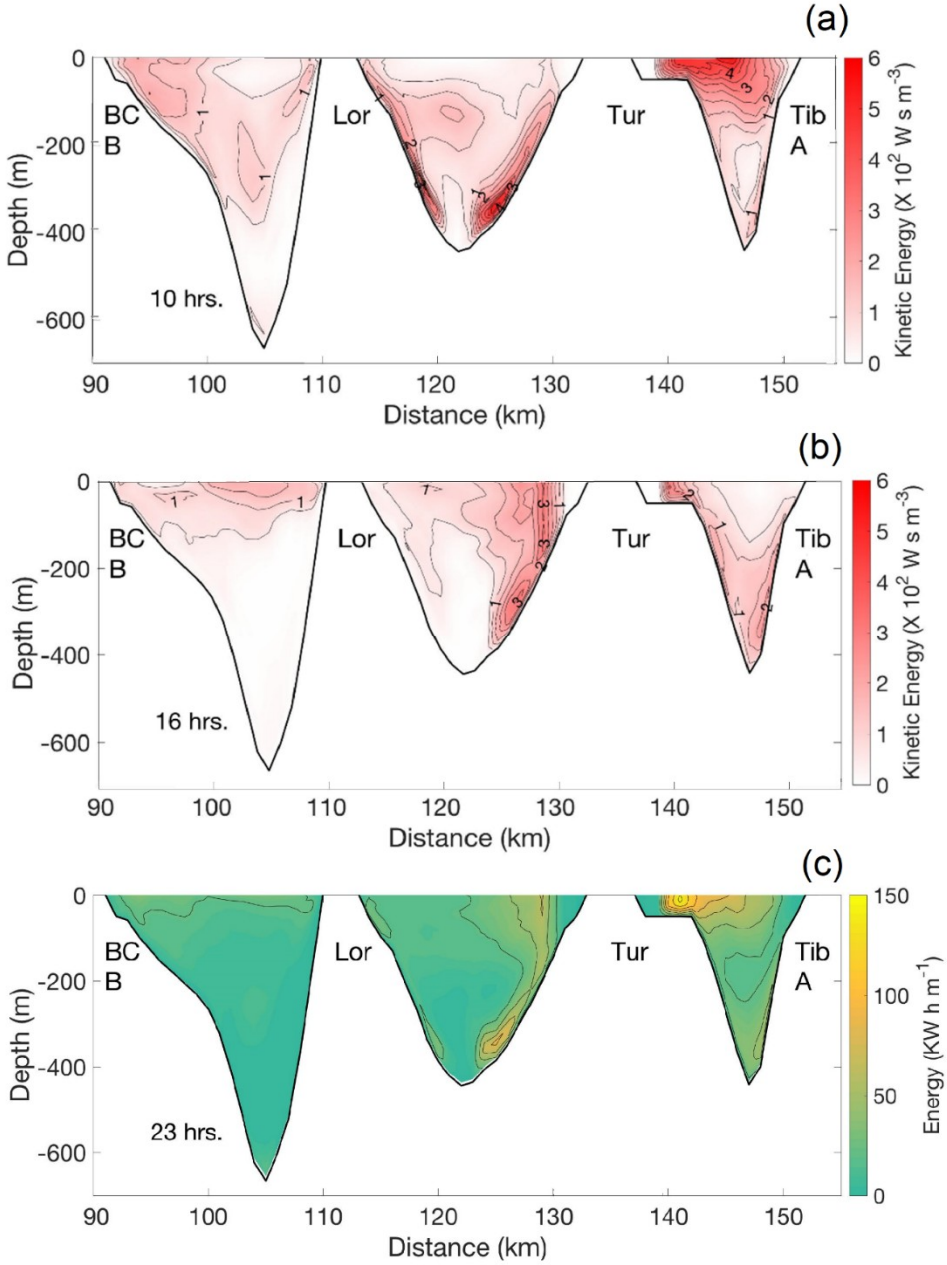

Figure 7. Same as Figure 5 but for kinetic energy (KE) for (**a**) inflow, (**b**) outflow. Panel (**c**) is the average tidal power density for a total tidal cycle.

4.2. Results of Field Measurements

When analyzing the model results of current velocities and kinetic energy values, we used the previously obtained data from a moored ADCP Nortek 400 kHz, which was placed north of the sill (Figures 1, 8 and 9) (details in [21]. The currents were measured every 4 m at 17 levels (from 80 to 12 m), with a time interval of 30 s. Horizontal currents were rotated in an angle of 30° to the u-axis, i.e., along the direction of the tidal flow from the sill to the northeast. This direction is shown by the bold dashed line in Figure 3a. During the measurements, the maximum velocity of the horizontal currents in the indicated water layer was approximately ± 0.6 ms^{-1}.

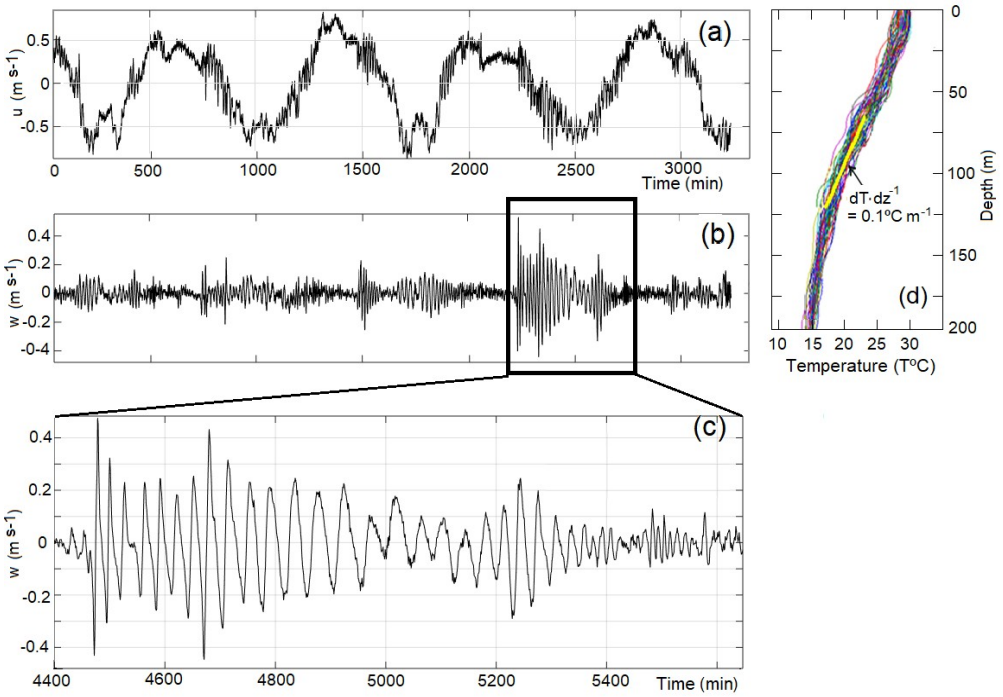

Figure 8. Measured currents at 62 m depth at mooring northeast of San Esteban Sill. (**a**) speed of the horizontal component v and (**b**) vertical component w of the current velocity. (**c**) a group of large-amplitude solitons (wave heights of 55–70 m, periods of 12–15 min). (**d**) Vertical temperature profiles measured near the mooring during the experiment (19 casts total).

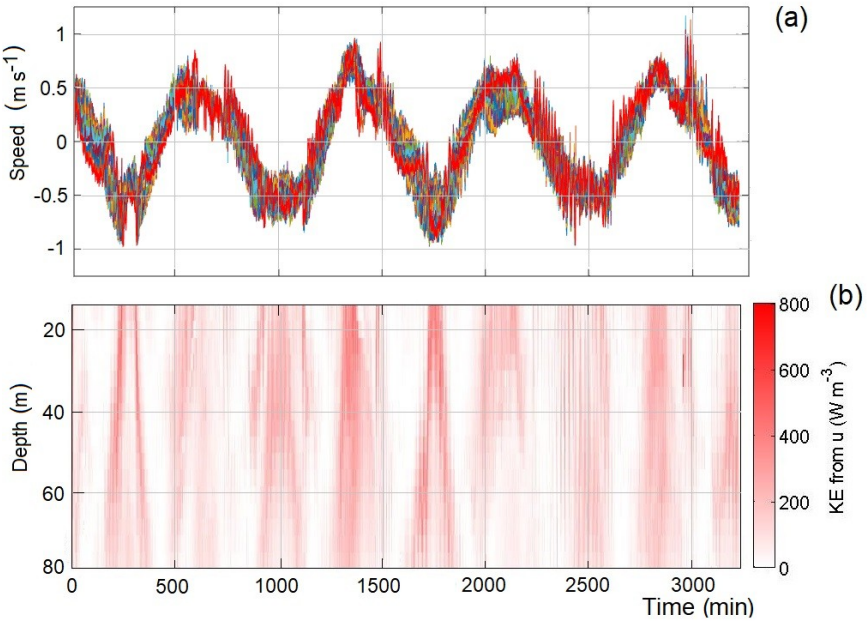

Figure 9. (**a**) u-component of the current velocity at 17 ADCP depths. (**b**) Total kinetic energy of the flow in this layer of water.

The horizontal and vertical components of currents at 62 m depth can be seen in Figure 8. The moving stream included barotropic and baroclinic components, which cannot be separated in our instrumental measurements, as this requires measurements in the entire water column from the surface to bottom. However, we can make some important estimates. As can be seen from Figure 8b, the baroclinic flow (vertical component of currents) caused

by dispersive internal waves is significant and when groups of nonlinear waves (solitons) pass the mooring, it reaches 30–40 cm s^{-1}, which is comparable to the barotropic flow.

The vertical displacements of water layers were calculated using the mooring data. This technique converts the time series of temperature into heights, for a determined depth, based on the relationship: $\Delta\zeta_z(t) = \zeta_z(t_1) - \zeta_z(t_0) = [T(t_1) - T(t_0)] / \left(\overline{dT/dz}\right)$, where $\zeta_z(t_1)$ and $\zeta_z(t_0)$ are vertical displacements at level z times t_1 and t_0, which originate temperature fluctuations $T(t_1)$, $T(t_0)$. $\left(\overline{dT/dz}\right)$ is the average vertical temperature gradient [20,30]. The average vertical temperature gradient was estimated using 3-h cast data from the ship's CTD SBE-19+ during the experiment.

Calculations have shown that the leading waves in the group have a height of over 70 m. They can be seen in the sea surface as smooth (divergence in the interior) and rough zones (convergence in the interior), with stripes 200–300 m wide, extending across the Gulf. They are also clearly visible in satellite imagery [2,3].

The horizontal flow velocities measured by the ADCP (Figure 9a) agree with the model data, and the vertical-temporal variability of the kinetic energy calculated in the measurement layers between 12 and 80 m levels (Figure 9b) also shows good agreement with the measured data.

5. Conclusions

We present numerical ocean modelling results of depth-characterized flows between the Midriff Islands in the Gulf of California, reported by many authors as potential zones for possible production of renewable energy [12].

The numerical domain covers the region of the Midriff Islands and is forced only with tidal flux, since it is the main forcing in the dynamics of the Gulf. The numerical model adequately reproduces the increase in speed in this region and the passage of internal wave patterns toward the lee of the islands during the inflow and outflow of the tidal semidiurnal cycle, showing the increase in kinetic energy. The velocities obtained with our three-dimensional model in the region are similar to those reported by [12]. Because this area has been identified as a region with great potential for the production of renewable energy, the temporal and depth characterization of flows that pass between the islands provided herein are critical to consider in alternative energy channeling deployments.

We define a section in depth between Tiburon Island (TI) and the Baja California (BC) coast that passes the Turón and San Lorenzo Islands (dashed line in Figure 2a), of approximate width of 56 km where the velocity values of the current lead to the calculation of the volumetric flows (Q) and the kinetic energy (KE). This section is where the tidal inflow and outflow increase in velocity producing large amounts of kinetic energy (KE).

Our model results show that the transport is not proportional to the transversal area of each section, with transport being greatest in Section II, with values of 1.75 Sv in inflow and 2.07 Sv in outflow, between Turón and San Lorenzo Islands.

The characterization of the along-gulf velocity component shows spatial differences for inflow and outflow. During the inflow, the highest velocity values are present in the surface to bottom core of Section II, and reach values of 0.8 m s^{-1}, while during the outflow, the highest velocity values are present in the surface core of Section II and the bottom core of Section I, with maximum values of 0.8 m s^{-1} as well. The lowest speeds are presented in Section III, near BC, with maximum values of 0.5 m s^{-1} in surface layers. Our in-situ measurements indicate that there are vertical movements of up to 70 m at 60 to 70 km distance from the islands. We consider that it is important to study the propagation of this energy associated with internal waves and to identify the process of evolution and dispersion of these waves towards the upper gulf. Although there is high energy in the area between the islands, the cores with the highest speed and kinetic energy are separated from the shoreline and the seabed. These results are important for the consideration of marine energy generation system installation.

Author Contributions: Conceptualization, F.A.V.-M. and A.F.; validation, F.A.V.-M. and A.F., formal analysis, F.A.V.-M. and A.F., data curation, A.F., writing—original draft preparation, F.A.V.-M. and A.F.; writing—review, editing and project administration, F.A.V.-M. and A.F. All authors have read and agreed to the published version of the manuscript.

Funding: This work was partially supported by the CONACYT project No.105622.

Institutional Review Board Statement: Not applicable.

Informed Consent Statement: Not applicable.

Data Availability Statement: Not applicable.

Acknowledgments: The work was supported by the Mexican National Council for Science and Technology (CONACYT), grant No. 35553-T. The authors gratefully acknowledge the help and technical assistance of M.Sc. students Diego Pantoja-Gonzalez, Edgar Flores-Chavez, Hector Santiago-Hernandez from the University of Guadalajara, as well as Carlos Vargas-Aguilera from CICESE. The authors also thank Lydia Betty Ladah for their help in editing this manuscript.

Conflicts of Interest: The authors declare no conflict of interest. The funders had no role in the design of the study; in the collection, analyses, or interpretation of data; in the writing of the manuscript, or in the decision to publish the results.

References

1. Badan-Dangon, A.; Hendershott, M.; Lavín, M.F. Underway Doppler current profiles in the Gulf of California. *Eos Trans. AGU* **1991**, *72*, 217–218.
2. Fu, L.-L.; Holt, B. Internal waves in the Gulf of California: Observations from a spaceborne radar. *J. Geophys. Res.* **1984**, *89*, 2053–2060. [CrossRef]
3. Apel, J.R.; Gonzalez, F.I. Nonlinear features of internal waves off Baja California as observed from the SEASAT imaging radar. *J. Geophys. Res.* **1983**, *88*, 4459–4466. [CrossRef]
4. Howell, T.L.; Brown, W.S. Nonlinear internal waves on the California continental shelf. *J. Geophys. Res.* **1985**, *90*, 7256–7264. [CrossRef]
5. Filonov, A.E. Internal tide and tsunami waves in the continentalshelf of the Mexican western coast. *Oceanogr. East. Pac.* **2000**, *1*, 31–45.
6. Filonov, A.E.; Konyaev, K.V. Nonlinear Internal Waves Near Mexico's Central Pacific Coast. In *Nonlinear Processes in Geophysical Fluid Dynamics*; Velasco Fuentes, O.U., Sheinbaum, J., Ochoa, J., Eds.; Springer: Berlin/Heidelberg, Germany, 2003. [CrossRef]
7. Filonov, A.; Novotryasov, V. Features of the nonlinear internal wave spectrum in the coastal zone. *Geophys. Res. Lett.* **2005**, *32*, L15602. [CrossRef]
8. AFilonov, A.; Novotryasov, V. On a spectrum of nonlinear internal waves in the oceanic coastal zone. *Nonlinear Process. Geophys.* **2007**, *14*, 757–762. [CrossRef]
9. Osborne, A.R.; Burch, T.L. Internal Solitons in the Andaman Sea. *Science* **1980**, *208*, 451–460. [CrossRef]
10. Da Silva, J.C.B.; Magalhaes, J.M. Internal solitons in the Andaman Sea: A new look at an old problem. In Proceedings of the Remote Sensing of the Ocean, Sea Ice, Coastal Waters, and Large Water Regions 2016, Edinburgh, UK, 19 October 2016; p. 999907. [CrossRef]
11. Magalhaes, J.M.; Da Silva, J.C.B. Internal Solitary Waves in the Andaman Sea: New Insights from SAR Imagery. *Remote Sens.* **2018**, *10*, 861. [CrossRef]
12. Magalhaes, J.M.; da Silva, J.C.B.; Buijsman, M.C. Long lived second mode internal solitary waves in the Andaman Sea. *Sci. Rep.* **2020**, *10*, 10234. [CrossRef]
13. Alpers, W.; Vlasenko, V. Internal Waves in the Andaman Sea. In *Remote Sensing of the Asian Seas*; Barale, V., Gade, M., Eds.; Springer: Cham, Switzerland, 2019. [CrossRef]
14. Apel, J.R.; Holbrook, J.R.; Liu, A.K.; Tsai, J.J. The Sulu Sea Internal Soliton Experiment. *J. Phys. Oceanogr.* **1985**, *15*, 1625–1651. [CrossRef]
15. Zeng, K.; Alpers, W. Generation of internal solitary waves in the Sulu Sea and their refraction by bottom topography studied by ERS SAR imagery and a numerical model. *Int. J. Remote. Sens.* **2004**, *25*, 1277–1281. [CrossRef]
16. Wunsch, C. Internal tides in the ocean. *Rev. Geophys.* **1975**, *13*, 167–182. [CrossRef]
17. Filonov, A.E.; Lavín, M.F. Internal tides in the Northern Gulf of California. *J. Geophys. Res.* **2003**, *108*, 3151. [CrossRef]
18. Paden, C.A.; Abbott, M.R.; Winant, C.D. Tidal and atmospheric forcing of the upper ocean in the Gulf of California: 1. Sea surface temperature variability. *J. Geophys. Res. Space Phys.* **1991**, *96*, 18337. [CrossRef]
19. Hendershott, M.; Speranza, A. Co-oscillating tides in long, narrow bays; the Taylor problem revisited. *Deep. Sea Res. Oceanogr. Abstr.* **1971**, *18*, 959–980. [CrossRef]
20. Filonov, A. Inclined internal tide waves at a narrow Mexican Pacific shelf. *Ocean Dyn.* **2011**, *61*, 917–931. [CrossRef]

21. Ruvalcaba-Aroche, E.D.; Filonov, A.; Sánchez-Velasco, L.; Ladah, L.B.; Cruz-Hernández, J. Internal tidal waves in Tiburon Basin (Gulf of California, Mexico) modulate fish larvae aggregations. *Cont. Shelf Res.* **2019**, *178*, 41–50. [CrossRef]
22. Filonov, A.; Tereshchenko, I.; Ladah, L.B.; Pantoja-Gonzalez, D.A.; Velázquez-Muñoz, F.A. High amplitude internal tidal waves generated over an underwater sill in the Gulf of California. *Cont. Shelf Res.* **2020**, *210*, 104290. [CrossRef]
23. Mejia-Olivares, C.J.; Haigh, I.; Wells, N.; Coles, D.S.; Lewis, M.; Neill, S.P. Tidal-stream energy resource characterization for the Gulf of California, México. *Energy* **2018**, *156*, 481–491. [CrossRef]
24. Magar, V.; Godínez, V.M.; Gross, M.S.; López-Mariscal, M.; Bermúdez-Romero, A.; Candela, J.; Zamudio, L. In-Stream Energy by Tidal and Wind-Driven Currents: An Analysis for the Gulf of California. *Energies* **2020**, *13*, 1095. [CrossRef]
25. Blumberg, A.F.; Mellor, G.L. A description of a three-dimensional coastal ocean circulation model. *Coastal Upwelling* **1987**, *4*, 1–16.
26. Argote, M.L.; Amador, A.; Lavín, M.F.; Hunter, J.R. Tidal dissipation and stratification in the Gulf of California. *J. Geophys. Res. Space Phys.* **1995**, *100*, 16103–16118. [CrossRef]
27. Carbajal, N.; Backhaus, J.O. Simulation of tides, residual flow and energy budget in the Gulf of California. *Oceanol. Acta* **1998**, *21*, 429–446. [CrossRef]
28. García-Silva, E.D.; Filonovb, A.; Sánchez-Velasco, L.; Ladah, L.B.; Cruz-Hernándeza, J. Marinone, Tidal dynamics and energy budget in the Gulf of California. *Cienc. Mar.* **2000**, *27*, 323–353. [CrossRef]
29. Marinone, S. Tidal currents in the gulf of california: Intercomparisons among two- and three-dimensional models with observations. *Cienc. Mar.* **2000**, *26*, 275–301. [CrossRef]
30. Konyaev, K.V.; Sabinin, K.D. *Waves Inside the Ocean (in Russian)*; Hydrometeoizdat: St.-Petersburg, Russia, 1992; p. 272.